Clinical Oral Investigations
https://doi.org/10.1007/s00784-021-04118-w

ORIGINAL ARTICLE

Comparison of calcium and hydroxyl ion release ability and in vivo apatite-forming ability of three bioceramic-containing root canal sealers

Razi Saifullah Ibn Belal[1] · Naoki Edanami[1] · Kunihiko Yoshiba[2] · Nagako Yoshiba[1] · Naoto Ohkura[1] · Shoji Takenaka[1] · Yuichiro Noiri[1]

Received: 30 April 2021 / Accepted: 30 July 2021

Abstract

Objective Bioceramic-containing root canal sealers promote periapical healing via Ca^{2+} and OH^- release and apatite formation on the surface. This study aimed to compare Ca^{2+} and OH^- release and in vivo apatite formation of three bioceramic-containing root canal sealers: EndoSequence BC sealer (Endo-BC), MTA Fillapex (MTA-F), and Nishika Canal Sealer BG (N-BG).

Materials and methods Polytetrafluoroethylene tubes filled with sealers were immersed in distilled water for 6 and 12 h and for 1, 7, 14, and 28 days to measure Ca^{2+} and OH^- release. Additionally, tubes filled with sealers were implanted in the backs of rats for 28 days, and in vivo apatite formation was analyzed using an electron probe microanalyzer.

Results Endo-BC released significantly more Ca^{2+} than the other sealers at 6 and 12 h and 1 day. Ca^{2+} release was significantly lower from N-BG than from Endo-BC and MTA-F at 14 and 28 days. OH^- release was significantly higher from Endo-BC than from the other sealers throughout the experiment, except at 1 day. OH^- release was lower from N-BG than from MTA-F at 6 h and 7 days. Only Endo-BC implants exhibited apatite-like calcium-, phosphorus-, oxygen-, and carbon-rich spherulites and apatite layer–like calcium- and phosphorus-rich, but radiopaque element-free, surface regions.

Conclusions Ca^{2+} and OH^- release is ranked as follows: Endo-BC > MTA-F > N-BG. Only Endo-BC demonstrated in vivo apatite formation.

Clinical relevance Endo-BC could promote faster periapical healing than MTA-F and N-BG.

Keywords Bioceramic-containing root canal sealer · Apatite-forming ability · Calcium ion release · Hydroxyl ion release · Subcutaneous implantation · Electron probe microanalyzer

Introduction

To achieve healing of periapical lesions with an endodontic origin, root canal filling using gutta-percha points with root canal sealer is performed after chemomechanical root canal preparation [1]. Recently, bioceramic-containing root canal sealers have attracted considerable attention owing to their distinctive bioactive properties.

Bioceramic-containing root canal sealers release Ca^{2+} and OH^- during and after setting [2, 3]. In addition, they produce bone-like apatite on the surface when they come into contact with phosphate-containing solutions such as interstitial tissue fluids [4]. Ca^{2+} stimulates osteogenic differentiation of bone marrow mesenchymal stem cells [5] and periodontal ligament stem cells [6] by upregulating osteopontin and bone morphogenic protein-2 expression, respectively. Likewise, OH^- increases the proliferation and mineralization of osteoblasts and cementoblasts [7, 8]. Furthermore, the bone-like apatite acts as a substrate for the attachment of cementoblasts and promotes cementum formation at the apical foramen [9]. Therefore, bioceramic-containing root canal

✉ Naoki Edanami
edanami@dent.niigata-u.ac.jp

[1] Division of Cariology, Operative Dentistry and Endodontics, Department of Oral Health Science, Niigata University Graduate School of Medical and Dental Sciences, 2-5274 Gakkocho-dori, Chuo-ku, Niigata 951-8514, Japan

[2] Division of Oral Science for Health Promotion, Department of Oral Health and Welfare, Niigata University Graduate School of Medical and Dental Sciences, Niigata, Japan

Published online: 16 August 2021

sealers not only seal the root canal system mechanically, but also accelerate periapical tissue healing biologically.

At present, various bioceramic-containing root canal sealers are commercially available. EndoSequence BC sealer (Endo-BC; Brasseler, Savannah, GA, USA) is a premixed injectable root canal sealer with calcium silicate as the bioceramic component. The setting of Endo-BC is achieved by precipitating a calcium silicate hydrate matrix in the presence of water [10]. MTA Fillapex (MTA-F; Angelus, Londrina, Brazil) is a resin-modified root canal sealer with a two-paste formulation that also contains calcium silicate as the bioceramic component. The mixed paste hardens on contact with water by the complexation of salicylate resin and calcium hydroxide. Calcium hydroxide is supplied by the hydration of calcium silicate in the sealer [10]. Nishika Canal Sealer BG (N-BG; Nippon Shika Yakuhin, Yamaguchi, Japan) is a recently marketed two-paste self-setting root canal sealer. Unlike the other two sealers, N-BG contains bioactive glass as the bioceramic component. After the two pastes have been mixed, N-BG sets via the reaction of magnesium oxide with fatty acids, without the need for water [2].

Considering the differences in composition and setting reactions, these sealers may have different Ca^{2+} and OH^- release and apatite-forming abilities. However, limited evidence is available regarding the differences, although the knowledge is needed for appropriate material selection by dental clinicians, especially under the current situation of insufficient clinical trials evaluating these sealers [11, 12]. While a few studies have compared the Ca^{2+} and OH^- release abilities of Endo-BC and MTA-F [13–15], none has compared the abilities of N-BG with that of Endo-BC or MTA-F. Furthermore, while previous studies showed that all three sealers produced apatite after immersion in inorganic artificial body fluids in vitro [4, 16, 17], their in vivo applications have not been evaluated. Therefore, this study sought to compare the three bioceramic-containing root canal sealers in terms of their Ca^{2+} and OH^- release abilities and in vivo apatite-forming ability.

Materials and methods

Analysis of Ca^{2+} and OH^- release ability

The specifications of the experimental sealers are presented in Table 1. The sealers were prepared according to the manufacturer's instructions and loaded into sterilized closed-end polytetrafluoroethylene tubes (length: 5 mm; inner diameter: 2 mm). The sealer-filled tubes ($n = 5$ for each sealer) were immediately immersed in 10 mL of distilled water (DW) and stored at 37 °C. The soaking water was collected and replaced at six time points (6 and 12 h, and 1, 7, 14, and 28 days). The Ca^{2+} and OH^- concentrations (pH) of the collected soaking water were measured using an inductively coupled plasma–atomic emission spectroscope (SPS1500; Seiko Instruments, Tokyo, Japan) and a pH meter (LAQUA TWIN; AS ONE, Osaka, Japan), respectively. The data were analyzed using one-way analysis of variance and post hoc Tukey's test, with a significance level of 5%.

The results showed that the Ca^{2+} and OH^- release ability of the tested materials in DW was significantly different. Thus, we further analyzed whether the differences were significant in a buffering solution with an ionic concentration similar to human blood plasma (simulated body fluid, SBF). The SBF was prepared according to ISO 23,317; thus, the Ca^{2+} concentration was 100.2 mg L^{-1} and the pH was 7.4 [18]. The analysis was performed in the same way as described above, but changing the soaking medium from 10 mL of DW to 5 mL of SBF. Observations were recorded at four time points (1, 7, 14, and 28 days).

Analysis of *in vivo* apatite-forming ability

The in vivo apatite-forming ability was evaluated as described in our previous study [19]. Four-week-old Wistar rats ($n = 8$) were anesthetized via intraperitoneal injection of 8% chloral hydrate (350 mg/kg). Three separate 5-mm-long incisions were made on the back of each animal, and the

Table 1 Composition of the sealers used in this study

Materials	Manufacturer	Composition
EndoSequence BC Sealer	Brasseler, Savannah, GA, USA	Zirconium oxide, Calcium silicates, Calcium phosphates monobasic, Calcium hydroxide, Filler and Thickening agents
MTA Fillapex	Angelus, Londrina, PR, Brazil	*Base:* Methyl salicylate, Butylene glycol, Colophony, Calcium tungstate, Fumed silica *Catalyst:* Pentaerythritol, Rosinate, P-Toluenesolfonamide, Titanium dioxide, Tricalcium silicate, Dicalcium silicate, Calcium oxide, Tricalcium aluminate, Fumed silica
NISHIKA Canal Sealer BG	Nippon Shika Yakuhin, Tokyo, Japan	*Paste A:* Fatty acid, Bismuth subcarbonate, Silicon dioxide *Paste B:* Magnesium oxide, Bioactive glass, Silicon dioxide

incisions were laterally extended to create surgical cavities. The sealer-filled tubes, which were prepared in the same manner as described above, were then inserted into the cavities, and the cavities were closed using a 4–0 silk thread (Mani, Tochigi, Japan). Twenty-eight days after the surgery, the animals were euthanized by anesthetic overdose, and the sealer-filled tubes were collected along with the surrounding tissue. The samples were divided into two groups. One group of samples ($n=4$ for each sealer) was immersed in 5.25% sodium hypochlorite solution to remove the soft tissue from the tubes and preserve the sealer surface. Then, the exposed sealer surfaces of the extracted tubes were gold-coated with an ion sputtering device (IC-50; Shimadzu, Kyoto, Japan), and analyzed for ultrastructure and elemental composition using an electron probe microanalyzer (EPMA1601; Shimadzu) equipped with observation functions for scanning electron microscopy and wavelength-dispersive X-ray spectroscopy. The scanning electron microscopy image and elemental composition were recorded at a representative area (100.7 × 75.5 µm) for each sample. The other group of samples ($n=4$ for each sealer) was fixed with 2.5% glutaraldehyde solution buffered with 60 mmol/L HEPES for 24 h at 4 ℃ and embedded into epoxy resin (EPON 812; Taab, Aldermaston, UK) after dehydration in increasing concentrations of ethanol solution and acetone. Then, the samples were longitudinally sectioned with a water-cooled diamond wheel saw (MC-201 N; Maruto, Tokyo, Japan) through the center of the tubes. After being polished with 2400-grit and 4000-grit SiC papers (Marumoto Struers KK, Tokyo, Japan), the cross-sectional surface was examined by elemental mapping analysis using EPMA1601 at an accelerating voltage of 15 kV with a 0.9-µm step size and 0.1-s sampling time. A representative area (230.4 × 230.4 µm) was evaluated for each sample.

As a positive control, sealers aged in an inorganic artificial body fluid (SBF prepared according to ISO23317 [18]) for 28 days at 37 °C were examined ($n=4$ for each sealer). SBF was renewed weekly. Sealers hardened by immersion in DW for 1 day at 37 °C were examined as a negative control ($n=4$ for each sealer).

Results

Ca^{2+} and OH^- release ability

Endo-BC released a significantly higher amount of Ca^{2+} than the other two sealers at earlier time points (6 and 12 h, and 1 day) in DW. At later time points (7, 14, and 28 days), Endo-BC and MTA-F exhibited similar rates of Ca^{2+} release in DW. The Ca^{2+} release ability of N-BG in DW was significantly lower than that of Endo-BC and MTA-F at 14 and 28 days (Table 2). The OH^- release ability of Endo-BC in DW was significantly higher than that of MTA-F and N-BG throughout the experiment, except at 1 day. Compared with MTA-F, N-BG showed significantly lower OH^- values at 6 h and 7 days in DW (Table 3). The Ca^{2+} concentrations of Endo-BC-immersed in SBF were significantly higher than those of MTA-F or N-BG-immersed in SBF throughout the experiment (Table 4). The pH of Endo-BC-immersed in SBF were significantly higher than those of MTA-F or N-BG-immersed in SBF at 1, 7, and 14 days (Table 5).

Table 2 Calcium ion release from the tested sealers (mg L^{-1})

Sealers	6 h	12 h	1 day	7 days	14 days	28 days
Endo-BC	51.20 ± 15.25^a	5.93 ± 2.06^a	7.52 ± 1.10^a	13.72 ± 1.01^a	13.52 ± 3.70^a	10.18 ± 2.20^a
MTA-F	2.90 ± 1.72^b	1.61 ± 0.81^b	3.37 ± 2.00^b	15.22 ± 7.78^a	14.46 ± 8.55^a	10.86 ± 1.76^a
N-BG	1.02 ± 0.50^b	1.62 ± 0.74^b	4.05 ± 1.86^b	9.31 ± 1.63^a	4.28 ± 0.79^b	5.42 ± 1.89^b

Data are shown as the mean ± SD of five samples. Means associated with different letters in each column are significantly different at $P<0.05$ (one-way ANOVA and post hoc Tukey's test). *Endo-BC*, EndoSequence BC sealer; *MTA-F*, MTA Fillapex; *N-BG*, Nishika Canal Sealer BG

Table 3 Hydroxyl ion release of the tested sealers (pH)

Sealers	6 h	12 h	1 day	7 days	14 days	28 days
Endo-BC	10.86 ± 0.24^a	9.84 ± 0.32^a	9.82 ± 0.49^a	10.73 ± 0.11^a	10.50 ± 0.06^a	10.58 ± 0.08^a
MTA-F	9.39 ± 0.27^b	9.22 ± 0.33^b	9.59 ± 0.57^a	10.43 ± 0.20^b	9.55 ± 0.05^b	9.40 ± 0.19^b
N-BG	8.60 ± 0.27^c	9.07 ± 0.22^b	9.44 ± 0.32^a	10.12 ± 0.13^c	9.60 ± 0.03^b	9.58 ± 0.02^b

Data are shown as the mean ± SD of five samples. Means associated with different letters in each column are significantly different at $P<0.05$ (one-way ANOVA and post hoc Tukey's test). *Endo-BC*, EndoSequence BC sealer; *MTA-F*, MTA Fillapex; *N-BG*, Nishika Canal Sealer BG

In vivo apatite-forming ability

Ultrastructural analysis revealed that the surface of SBF-immersed positive-control sealers exhibited an apatite-like spherical structure (Fig. 1a, d, g), whereas the surface of DW-immersed negative-control sealers did not (Fig. 1b, e, h). The in vivo–implanted Endo-BC displayed apatite-like spherulites on the surface (Fig. 1c), whereas the in vivo–implanted MTA-F and N-BG displayed no spherulites (Fig. 1f, i). The average surface elemental composition of the four samples in each experimental condition is shown in Fig. 1j-l. The apatite-like spherulites formed on SBF-immersed sealers and in vivo–implanted Endo-BC were carbon-rich and composed of calcium, phosphorus, and oxygen (Fig. 1j-l). In vivo–implanted N-BG also displayed a calcium-, phosphorus-, oxygen-, and carbon-rich surface; however, it had a certain amount of bismuth on the surface as did the DW-immersed N-BG (Fig. 1l). In the cross-section elemental mapping analysis, the SBF-immersed positive-control sealers (Fig. 2a1-c4) and the in vivo–implanted Endo-BC (Fig. 3a1-a4) showed apatite layer–like calcium- and phosphorus-rich, but radiopaque element (zirconium, titanium, or bismuth)-free, regions; the DW-immersed negative-control sealers (Fig. 2d1-f4) and the in vivo–implanted MTA-F and N-BG (Fig. 3b1-c4) showed no such regions. The elemental mapping analysis showed the area of silicon element depletion inside the in vivo–implanted N-BG (Supplementary Fig. 1).

Discussion

This study demonstrated that the relative Ca^{2+} and OH^- release ability of the tested sealers in DW could be ranked as follows: Endo-BC > MTA-F > N-BG (Tables 2 and 3). Previous studies have demonstrated that Endo-BC releases higher Ca^{2+} and OH^- than MTA-F [13–15], which is in agreement with our findings. Although no previous studies have compared the Ca^{2+} and OH^- release properties of bioactive glass-type N-BG with those of calcium silicate–type Endo-BC and MTA-F, a recent study reported that N-BG released significantly lower amounts of Ca^{2+} than two calcium silicate–type bioceramic-containing root canal sealers [20], which is consistent with our findings. In this study, we further found that Endo-BC increased the Ca^{2+} concentration and pH of an artificial body fluid (SBF) to a significantly greater extent than did MTA-F and N-BG (Tables 4 and 5). Therefore, Endo-BC may stimulate apical tissue healing more than MTA-F and N-BG via higher Ca^{2+} and OH^- release, although further confirmation by cell culture study or animal study is necessary [21].

The differences in ion release may be largely due to the differences in type and proportion of the bioceramic components inside the sealers. The bioceramic component in both Endo-BC and MTA-F is calcium silicate, which produces calcium hydroxide on hydration. Calcium hydroxide, in turn, further dissociates into Ca^{2+} and OH^- in solution [22]. Meanwhile, the bioceramic component in N-BG is bioactive glass. The dissolution of bioactive glass increases the Ca^{2+} and OH^- concentrations in the surrounding environment [23]. Based on previous studies, the dissolution of bioactive glass may not produce Ca^{2+} and OH^- as abundantly as calcium silicate on hydration [24–26]. Regarding the proportion of bioceramic components, the manufacturers claim that Endo-BC contains approximately 50% calcium silicate, whereas MTA-F contains < 13.2% calcium silicate. The proportion of the bioactive glass component in N-BG is not disclosed; however, the sealer has a dual paste formulation and the bioactive glass is present only in paste B along with other non-bioceramic components (Table 1). Therefore, the proportion of the bioactive glass in N-BG is likely low.

Setting time and solubility may also be associated with differences in ion release ability. According to the

Table 5 pH of simulated body fluid after immersion of tested sealers

Sealers	1 day	7 days	14 days	28 days
Endo-BC	7.37 ± 0.05^a	7.45 ± 0.02^a	7.21 ± 0.04^a	6.96 ± 0.04^a
MTA-F	7.05 ± 0.02^b	7.15 ± 0.04^b	7.02 ± 0.03^b	6.96 ± 0.02^a
N-BG	7.05 ± 0.02^b	7.11 ± 0.02^b	7.04 ± 0.03^b	6.97 ± 0.01^a

Data are shown as the mean ± SD of five samples. Means associated with different letters in each column are significantly different at $P < 0.05$ (one-way ANOVA and post hoc Tukey's test). *Endo-BC*, EndoSequence BC sealer; *MTA-F*, MTA Fillapex; *N-BG*, Nishika Canal Sealer BG

Table 4 Calcium ion concentration of simulated body fluid after immersion of tested sealers (mg L^{-1})

Sealers	1 day	7 days	14 days	28 days
Endo-BC	210.74 ± 21.59^a	192.32 ± 10.82^a	145.28 ± 18.82^a	121.32 ± 9.66^a
MTA-F	105.37 ± 6.26^b	99.64 ± 2.56^b	97.05 ± 2.91^b	101.84 ± 2.27^b
N-BG	106.80 ± 1.58^b	99.07 ± 2.58^b	91.63 ± 1.79^b	95.69 ± 2.34^b

Data are shown as the mean ± SD of five samples. Means associated with different letters in each column are significantly different at $P < 0.05$ (one-way ANOVA and post hoc Tukey's test). *Endo-BC*, EndoSequence BC sealer; *MTA-F*, MTA Fillapex; *N-BG*, Nishika Canal Sealer BG

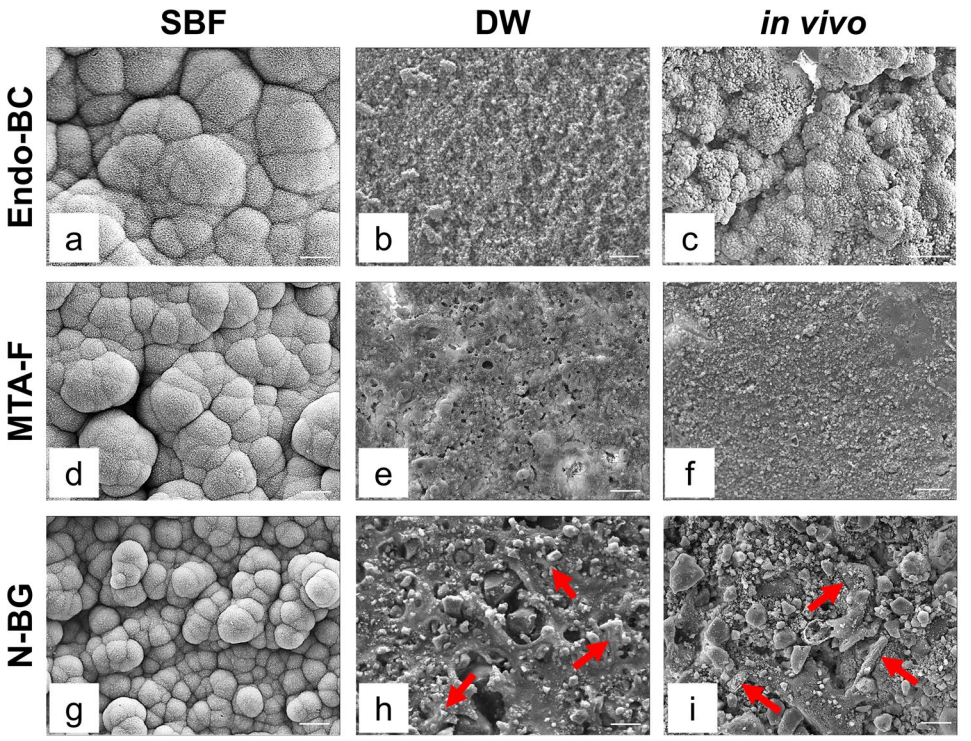

(j) Endo-BC

Elements	mol %		
	SBF	DW	*in vivo*
Ca	17.8	11.5	18.7
P	13.1	1.0	15.0
O	55.6	49.7	44.4
C	11.2	14.6	17.2
Si	0.0	6.4	0.0
Zr	0.0	16.3	0.6
others	2.4	0.6	4.0

(k) MTA-F

Elements	mol %		
	SBF	DW	*in vivo*
Ca	20.9	6.5	12.6
P	15.9	0.0	4.5
O	48.3	29.4	38.7
C	11.5	47.3	28.6
Si	0.2	7.0	5.1
Ti	0.0	1.9	1.5
others	3.1	8.0	9.1

(l) N-BG

Elements	mol %		
	SBF	DW	*in vivo*
Ca	18.6	6.6	18.2
P	16.1	2.9	15.0
O	50.6	35.2	42.1
C	11.0	41.9	17.4
Si	0.5	7.5	0.1
Bi	0.0	3.0	2.6
others	3.2	3.1	4.7

Fig. 1 Ultrastructure (a–i) and elemental composition (j–l) of the surface of EndoSequence BC sealer (Endo-BC) (a–c, j), MTA Fillapex (MTA-F) (d–f, k), and Nishika Canal Sealer BG (N-BG) (g–i, l) immersed in simulated body fluid (SBF) or distilled water (DW) or implanted in vivo. Apatite-like spherical structures are present on the surface of SBF-immersed positive control samples (a, d, g) and in vivo–implanted Endo-BC (c) but absent on the surface of DW-immersed negative control samples (b, e, h) and in vivo–implanted MTA-F (f) and N-BG (i). Bismuth subcarbonate–like rod-shaped crystals (arrows) are evident on the surface of DW-immersed and in vivo–implanted N-BG (h, i). The apatite-like spherulites are calcium (Ca)-, phosphorus (P)-, oxygen (O)-, and carbon (C)-rich (j–l). Si, silicon; Zr, zirconium; Ti, titanium; Bi, bismuth. Scale = 10 μm

manufacturer's instructions, the setting time of Endo-BC is 4 h, that of MTA-F is 2.5 h, and that of N-BG is 1 h. After setting, ion exchange between materials and the surrounding environment is restricted [13]. The degree of solubility of the sealers had been previously ranked as follows: Endo-BC > MTA-F > N-BG [2, 15]. Considering that these sealers release Ca^{2+} and OH^- because of the dissolution of their components, materials with higher solubilities presumably have higher Ca^{2+} and OH^- release abilities. It should be mentioned here that these orders of setting time and solubility are consistent with the order of ion release shown in this study.

This study evaluated the in vivo apatite-forming ability of three sealers by implanting the materials in rat subcutaneous tissue, which is a departure from the typical clinical situation, in which the sealers come in contact with periodontal ligament. However, periodontal ligament spontaneously produces calcified substances such as bone or cementum, which hinders the detection of bone-like apatite derived from chemical interactions between the sealers and body fluids. Furthermore, evaluating in vivo apatite-forming ability in human teeth is ethically inappropriate because it would require tooth extraction. Therefore, the rat subcutaneous implantation model is optimal for this purpose.

In our previous study, apatite formation on endodontic bioceramic materials started within 7 days after rat subcutaneous implantation [19]; thus, the 28-day observation period in this study provided ample time for evaluating the in vivo apatite-forming ability. This study showed that only Endo-BC implants displayed calcium-, phosphorus-, oxygen-, and carbon-rich spherulites and calcium- and phosphorus-rich but radiopaque element-free regions on the surface (Figs. 1 and 2). Previous studies reported that bone-like apatite formed on bioceramic materials exhibits a spherical appearance [27] and is composed of calcium, phosphorus, oxygen, and carbon [28]. Therefore, our findings indicated that Endo-BC possessed in vivo apatite-forming ability, whereas MTA-F and N-BG did not.

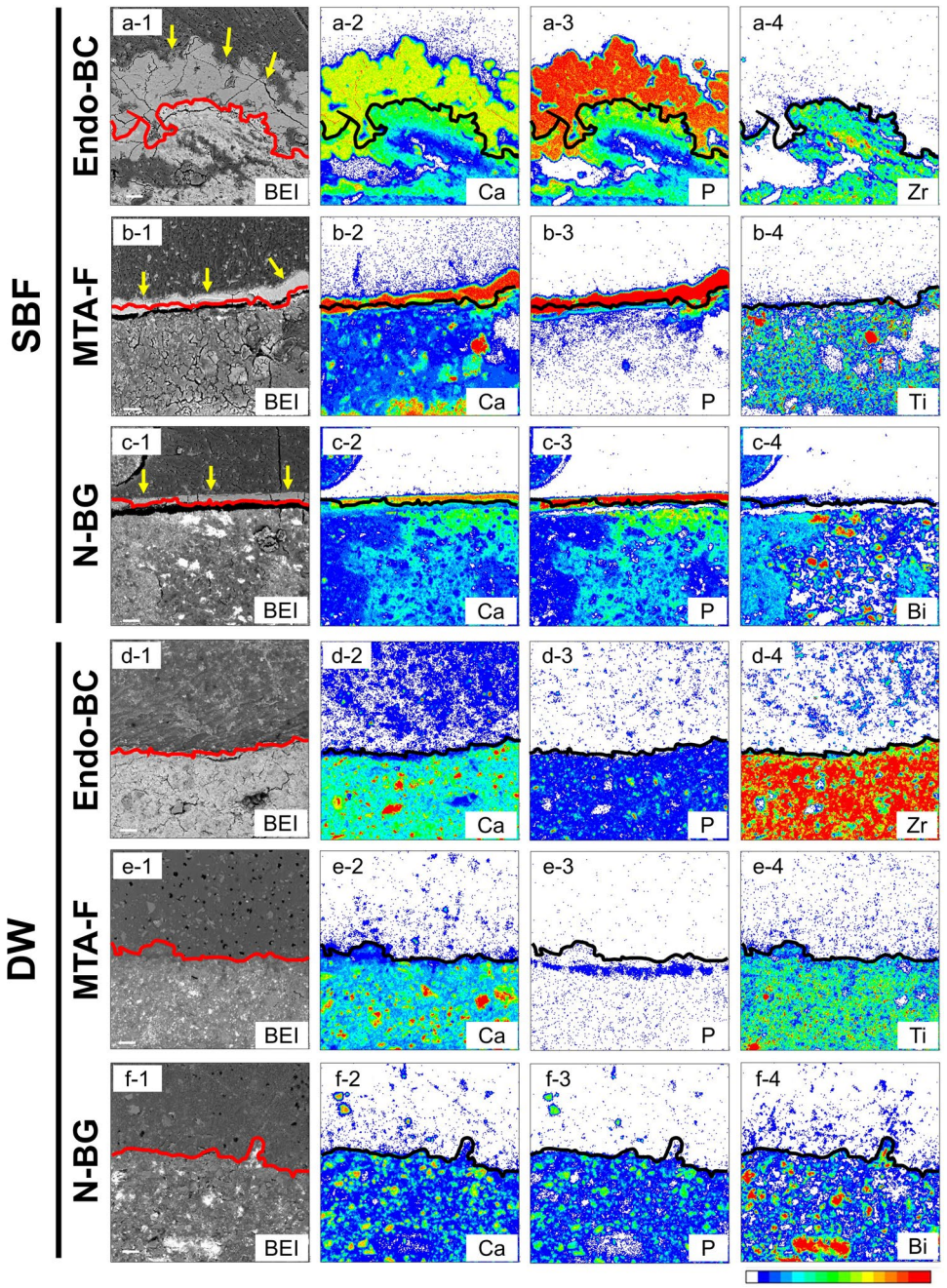

Fig. 2 Backscattered electron images (BEI) and elemental mapping images of the cross-sectioned EndoSequence BC sealer (Endo-BC) (a1–a4, d1–d4), MTA Fillapex (MTA-F) (b1–b4, e1–e4), and Nishika Canal Sealer BG (N-BG) (c1–c4, f1–f4) immersed in simulated body fluid (SBF) (a1–c4) or distilled water (DW) (d1–f4). Arrows in BEI images indicate an apatite layer–like region, which is calcium (Ca)- and phosphorus (P)-rich but radiopaque element-free. The apatite layer–like region is present on the surface of SBF-immersed positive control samples (a1–c4) but absent on the surface of DW-immersed negative control samples (d1–f4). Lines indicate the interface between the radiopaque element-positive and element-negative regions. The colored bar indicates the intensity of the elements, with red for higher and white for lower intensities. Zr, zirconium; Ti, titanium; and Bi, bismuth. Scale = 20 μm

In this study, N-BG implants also exhibited a calcium-, phosphorus-, oxygen-, and carbon-rich surface (Fig. 1). However, 2.6% of bismuth element and bismuth subcarbonate–like rod-shaped crystals were observed on the surface of N-BG implants (Fig. 1). Furthermore, no apatite-like spherulites or apatite layer–like regions were detected on the N-BG implants (Figs. 1 and 2). Therefore, the elemental composition change of the N-BG surface after in vivo implantation did not result from the surface being covered by apatite precipitate. We showed that an area of silicon element depletion was present inside the N-BG implants, suggesting that a massive amount of silicon ion was released from N-BG implants (Supplementary Fig. 1). Ion exchange between N-BG implants and the surrounding environment might have caused the elemental composition change.

Previous in vitro studies showed that the three tested sealers produced apatite in inorganic artificial body fluids [4, 16, 17]. We also confirmed these previous findings using SBF (Figs. 1 and 3). However, MTA-F and N-BG did not produce apatite-like precipitates in vivo. Two previous studies have also shown that in vitro tests using inorganic artificial body fluids cannot accurately estimate the in vivo apatite-forming

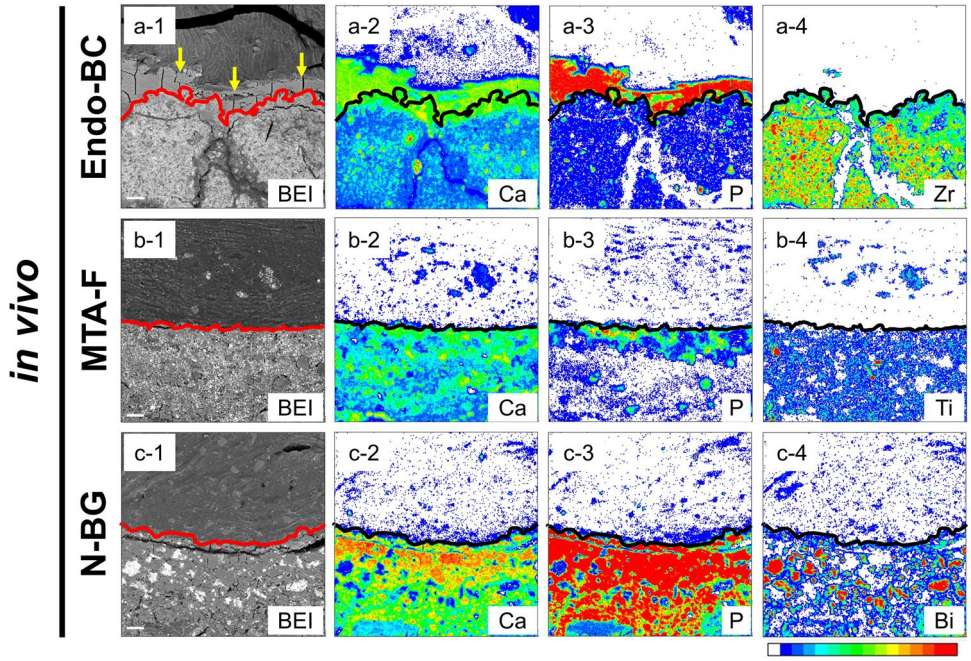

Fig. 3 Backscattered electron images (BEI) and elemental mapping images of the cross-sectioned EndoSequence BC sealer (Endo-BC) (a1–a4), MTA Fillapex (MTA-F) (b1–b4), and Nishika Canal Sealer BG (N-BG) (c1–c4) after in vivo implantation. Arrows in BEI images indicate an apatite layer–like region, which is calcium (Ca)- and phosphorus (P)-rich but radiopaque element-free. The apatite layer–like region is present on the surface of in vivo–implanted Endo-BC (a1–a4) but absent on the surface of in vivo–implanted MTA-F (b1–b4) and N-BG (c1–c4). Lines indicate the interface between the radiopaque element-positive and element-negative regions. The colored bar indicates the intensity of the elements, with red for higher and white for lower intensities. Zr, zirconium; Ti, titanium; and Bi, bismuth. Scale = 20 μm

ability of endodontic bioceramic materials [29, 30], possibly because of the presence of serum proteins in vivo. Serum proteins, represented by albumin, have been demonstrated to suppress apatite formation on bioceramic materials by reducing free calcium and phosphate ions in body fluids [31] and obscuring the apatite nucleation site on bioceramic materials [32].

It remains unclear why Endo-BC promotes apatite formation in vivo but MTA-F and N-BG do not. One possible reason is that the superior Ca^{2+} and OH^- release ability of Endo-BC enables apatite formation even in vivo. Ca^{2+} and OH^- induce apatite formation by increasing the supersaturation of the surrounding environment toward apatite precipitation [33]. Another possible reason is that a large amount of protein adsorption hinders the in vivo apatite-forming abilities of MTA-F and N-BG. Serum proteins, which negatively affect apatite nucleation on the bioceramic materials, as mentioned above, are more readily adsorbed on a hydrophobic surface than on a hydrophilic surface [34]. Indeed, the hydrophobicity of resin-containing MTA-F is higher than that of Endo-BC [35]. In addition, N-BG presumably has high hydrophobicity because it contains hydrophobic fatty acids [36] (Table 1). These possibilities will be the subject of future studies.

Conclusion

In conclusion, Endo-BC released a significantly higher amount of Ca^{2+} and OH^- than MTA-F and N-BG. Additionally, only Endo-BC formed apatite-like precipitates on the surface after rat subcutaneous implantation. These findings suggest that Endo-BC is a preferable material to MTA-F and N-BG in terms of bioactive properties. In the future, the extent to which the differences in ion release and apatite-forming abilities influence clinical outcomes should be investigated to obtain more authoritative evidence for optimal material selection.

Supplementary Information The online version contains supplementary material available at https://doi.org/10.1007/s00784-021-04118-w.

Acknowledgements This work was the result of using research equipment in CCRF, Niigata University. We thank Ms. Ayako Ikarashi for providing technical support. We thank Edanz Group (https://en-author-services.edanz.com/ac) for editing a draft of this manuscript.

Author contribution RSI Belal and N Edanami contributed to the conception, design, data acquisition, analysis, and interpretation, and drafted and critically revised the manuscript. N Yoshiba, N Ohkura, and S Takenaka contributed to data acquisition and critically revised the manuscript. K Yoshiba and Y Noiri contributed to data interpretation and critically revised the manuscript.

Funding The work was supported by Grants-in-Aid for Scientific Research from the Japan Society for the Promotion of Science (no. 19K19020 to N.E.).

Declarations

Ethics approval All experiments were reviewed and approved by the Committee on the Guidelines for Animal Experimentation of Niigata University (approval number: SA 00365). All applicable international, national, and/or institutional guidelines for the care and use of animals were followed.

Informed consent For this type of study, formal consent is not required.

Conflict of interest The authors declare no competing interests.

References

1. Schilder H (1974) Cleaning and shaping the root canal. Dent Clin North Am 18:269–296
2. Washio A, Morotomi T, Yoshii S, Kitamura C (2019) Bioactive glass-based endodontic sealer as a promising root canal filling material without semisolid core materials. Materials 12:3967. https://doi.org/10.3390/ma12233967
3. Trope M, Bunes A, Debelian G (2015) Root filling materials and techniques: bioceramics a new hope? Endod Top 32:86–96. https://doi.org/10.1111/etp.12074
4. Zamparini F, Siboni F, Prati C, Taddei P, Gandolfi MG (2019) Properties of calcium silicate-monobasic calcium phosphate materials for endodontics containing tantalum pentoxide and zirconium oxide. Clin Oral Investig 23:445–457. https://doi.org/10.1007/s00784-018-2453-7
5. Lee MN, Hwang HS, Oh SH, Roshanzadeh A, Kim JW, Song JH, Kim ES, Koh JT (2018) Elevated extracellular calcium ions promote proliferation and migration of mesenchymal stem cells via increasing osteopontin expression. Exp Mol Med 50:1–16. https://doi.org/10.1038/s12276-018-0170-6
6. Maeda H, Nakano T, Tomokiyo A, Fujii S, Wada N, Monnouchi S, Hori K, Akamine A (2010) Mineral trioxide aggregate induces bone morphogenetic protein-2 expression and calcification in human periodontal ligament cells. J Endod 36:647–652. https://doi.org/10.1016/j.joen.2009.12.024
7. Galow AM, Rebl A, Koczan D, Bonk SM, Baumann W, Gimsa J (2017) Increased osteoblast viability at alkaline pH in vitro provides a new perspective on bone regeneration. Biochem Biophys Reports 10:17–25. https://doi.org/10.1016/j.bbrep.2017.02.001
8. Muramatsu T, Kashiwagi S, Ishizuka H, Matsuura Y, Furusawa M, Kimura M, Shibukawa Y (2019) Alkaline extracellular conditions promote the proliferation and mineralization of a human cementoblast cell line. Int Endod J 52:639–645. https://doi.org/10.1111/iej.13044
9. Ricucci D, Grande NM, Plotino G, Tay FR (2020) Histologic response of human pulp and periapical tissues to tricalcium silicate–based materials: a series of successfully treated cases. J Endod 46:307–317. https://doi.org/10.1016/j.joen.2019.10.032
10. Komabayashi T, Colmenar D, Cvach N, Bhat A, Primus C, Imai Y (2020) Comprehensive review of current endodontic sealers. Dent Mater J 39:703–720. https://doi.org/10.4012/dmj.2019-288
11. Washio A, Miura H, Morotomi T, Ichimaru-Suematsu M, Miyahara H, Hanada-Miyahara K, Yoshii S, Murata K, Takakura N, Akao E, Fujimoto M, Matsuyama A, Kitamura C (2020) Effect of bioactive glass-based root canal sealer on the incidence of postoperative pain after root canal obturation. Int J Environ Res Public Health 17:8857. https://doi.org/10.3390/ijerph17238857
12. Aslan T, Dönmez Özkan H (2021) The effect of two calcium silicate-based and one epoxy resin-based root canal sealer on postoperative pain: a randomized controlled trial. Int Endod J 54:190–197. https://doi.org/10.1111/iej.13411
13. Lee JK, Kwak SW, Ha JH, Lee W, Kim HC (2017) Physicochemical properties of epoxy resin-based and bioceramic-based root canal sealers. Bioinorg Chem Appl 2017:25828492017. https://doi.org/10.1155/2017/2582849
14. Xuereb M, Vella P, Damidot D, Sammut CV, Camilleri J (2015) In situ assessment of the setting of tricalcium silicate-based sealers using a dentin pressure model. J Endod 41:111–124. https://doi.org/10.1016/j.joen.2014.09.015
15. Zhou HM, Shen Y, Zheng W, Li L, Zheng YF, Haapasalo M (2013) Physical properties of 5 root canal sealers. J Endod 39:1281–1286. https://doi.org/10.1016/j.joen.2013.06.012
16. Hanada K, Morotomi T, Washio A, Yada N, Matsuo K, Teshima H, Yokota K, Kitamura C (2019) In vitro and in vivo effects of a novel bioactive glass-based cement used as a direct pulp capping agent. J Biomed Mater Res - Part B Appl Biomater 107:161–168. https://doi.org/10.1002/jbm.b.34107
17. Siboni F, Taddei P, Zamparini F, Prati C, Gandolfi MG (2017) Properties of bioroot RCS, a tricalcium silicate endodontic sealer modified with povidone and polycarboxylate. Int Endod J 50:e120–e136. https://doi.org/10.1111/iej.12856
18. International Organization for Standardization (2014) International standard: ISO 23317:2014(E) Implants for surgery—In vitro evaluation for apatite-forming ability of implant materials. ISO, Geneva. https://www.iso.org/obp/ui/#iso:std:iso:23317:ed-3:v1:en
19. Hinata G, Yoshiba K, Han L, Edanami N, Yoshiba N, Okiji T (2017) Bioactivity and biomineralization ability of calcium silicate-based pulp-capping materials after subcutaneous implantation. Int Endod J 50:e40–e51. https://doi.org/10.1111/iej.12802
20. Bin JS, Kim HK, Lee HN, Kim YJ, Patel KD, Knowles JC, Lee JH, Song M (2020) Physical properties and biofunctionalities of bioactive root canal sealers in vitro. Nanomaterials 10:1–19. https://doi.org/10.3390/nano10091750
21. Braga RR, About I (2019) How far do calcium release measurements properly reflect its multiple roles in dental tissue mineralization? Clin Oral Investig 23:501. https://doi.org/10.1007/s00784-018-2789-z
22. Camilleri J (2007) Hydration mechanisms of mineral trioxide aggregate. Int Endod J 40:462–470. https://doi.org/10.1111/j.1365-2591.2007.01248.x
23. Hench LL (1991) Bioceramics: from concept to clinic. J Am Ceram Soc 74:1487–1510. https://doi.org/10.1111/j.1151-2916.1991.tb07132.x
24. Ohtsuki C, Kokubo T, Yamamuro T (1992) Mechanism of apatite formation on CaO-SiO2-P2O5 glasses in a simulated body fluid. J Non Cryst Solids 143:84–92. https://doi.org/10.1016/S0022-3093(05)80556-3
25. Jones JR, Sepulveda P, Hench LL (2001) Dose-dependent behavior of bioactive glass dissolution. J Biomed Mater Res 58:720–726. https://doi.org/10.1002/jbm.10053

26. Formosa LM, Mallia B, Bull T, Camilleri J (2012) The microstructure and surface morphology of radiopaque tricalcium silicate cement exposed to different curing conditions. Dent Mater 28:584–595. https://doi.org/10.1016/j.dental.2012.02.006
27. Han L, Okiji T, Okawa S (2010) Morphological and chemical analysis of different precipitates on mineral trioxide aggregate immersed in different fluids. Dent Mater J 29:512–517. https://doi.org/10.4012/dmj.2009-133
28. Kim HM, Himeno T, Kokubo T, Nakamura T (2005) Process and kinetics of bonelike apatite formation on sintered hydroxyapatite in a simulated body fluid. Biomaterials 26:4366–4373. https://doi.org/10.1016/j.biomaterials.2004.11.022
29. Meschi N, Li X, Van Gorp G, Camilleri J, Van Meerbeek B, Lambrechts P (2019) Bioactivity potential of Portland cement in regenerative endodontic procedures: from clinic to lab. Dent Mater 35:1342–1350. https://doi.org/10.1016/j.dental.2019.07.004
30. Moinzadeh AT, Aznar Portoles C, Schembri Wismayer P, Camilleri J (2016) Bioactivity potential of endo sequence BC RRM putty. J Endod 42:615–621. https://doi.org/10.1016/j.joen.2015.12.004
31. Wang K, Leng Y, Lu X, Ren F, Ge X, Ding Y (2012) Theoretical analysis of protein effects on calcium phosphate precipitation in simulated body fluid. CrystEngComm 14:5870–5878. https://doi.org/10.1039/c2ce25216c
32. Tagaya M, Ikoma T, Takeguchi M, Hanagata N, Tanaka J (2011) Interfacial serum protein effect on biological apatite growth. J Phys Chem C 115:22523–22533. https://doi.org/10.1021/jp208104z
33. Lu X, Leng Y (2005) Theoretical analysis of calcium phosphate precipitation in simulated body fluid. Biomaterials 26:1097–1108. https://doi.org/10.1016/j.biomaterials.2004.05.034
34. Wang K, Zhou C, Hong Y, Zhang X (2012) A review of protein adsorption on bioceramics. Interface Focus 2:259–277. https://doi.org/10.1098/rsfs.2012.0012
35. Ha JH, Kim HC, Kim YK, Kwon TY (2018) An evaluation of wetting and adhesion of three bioceramic root canal sealers to intraradicular human dentin. Materials 11:1286. https://doi.org/10.3390/ma11081286
36. Liu P, Feng C, Wang F, Gao Y, Yang J, Zhang W, Yang L (2018) Hydrophobic and water-resisting behavior of Portland cement incorporated by oleic acid modified fly ash. Mater Struct Constr 51:1–9. https://doi.org/10.1617/s11527-018-1161-8